

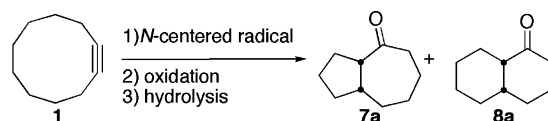
N-Centered Radicals in Self-Terminating Radical Cyclizations: Experimental and Computational Studies

Uta Wille,^{*,†,‡} Gerold Heuger,^{†,‡} and Christian Jargstorff[§]

School of Chemistry/BIO21 Molecular Science and Biotechnology Institute, The University of Melbourne, 30 Flemington Road, Parkville, Victoria 3010, Australia, ARC Centre of Excellence for Free Radical Chemistry and Biotechnology, Otto-Diels Institut für Organische Chemie, Christian-Albrechts Universität Kiel, Olshausenstrasse 40, 24098 Kiel, Germany

uwille@unimelb.edu.au

Received October 21, 2007



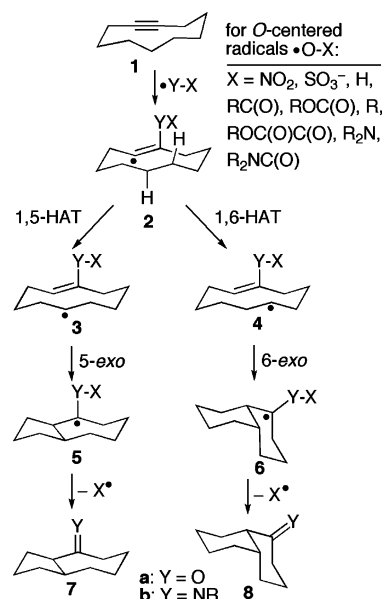
Intermolecular addition of photochemically generated *N*-centered aminium and amidyl radicals **13a–d** and **16a,b**, respectively, to the cyclic alkyne **1** initiates a radical translocation/cyclization cascade, followed by an oxidative termination step that eventually leads to formation of the bicyclic ketones **7a** and **8a**. Computational studies were performed to gain insight into the mechanism of these reactions, which are an interesting modification of the recently discovered concept of self-terminating radical cyclizations.

Introduction

Oxidation reactions performed under mild and heavy metal free conditions are a highly desirable goal in synthetic organic chemistry. Self-terminating radical cyclizations are a new concept in radical chemistry recently discovered by us: C≡C triple bonds in cyclic and open-chain alkynes are transformed into ketones under mild conditions in a radical addition/cyclization sequence using *O*-centered radicals of type XO• as oxidant.¹ The assumed mechanism is shown in Scheme 1 for the exemplary reaction of cyclodecyne **1** (with Y = O).

The initially formed vinyl radical **2a** undergoes a transannular 1,5 or 1,6 hydrogen atom transfer (HAT), **2a** → **3a/4a**, followed by a 5- or 6-*exo* radical cyclization, **3a/4a** → **5a/6a**, respectively. Homolytic cleavage of the O–X bond in the final step leads to the isomeric cis-fused bicyclic ketones **7a** and **8a** with simultaneous release of a radical X•. Since X• does not act as a radical chain carrier, this sequence can be regarded as a “self-

SCHEME 1



terminating, oxidative radical cyclization”, in which XO• represents a synthon for *O* atoms in solution.

Since the initial discovery of self-terminating radical oxygenations a decade ago using the *O*-centered nitrate radical, NO₃• (X = NO₂), we have shown that this sequence represents a general concept that can be applied to every major class of

[†] The University of Melbourne.

[‡] ARC Centre of Excellence for Free Radical Chemistry and Biotechnology.

[§] Christian-Albrechts Universität Kiel.

(1) (a) Wille, U.; Plath, C. *Liebigs Ann./Recl.* **1997**, 111. (b) Wille, U.; Lietzau, L. *Tetrahedron* **1999**, *55*, 10119. (c) Wille, U.; Lietzau, L. *Tetrahedron* **1999**, *55*, 11456. (d) Lietzau, L.; Wille, U. *Heterocycles* **2001**, *55*, 377. (e) Wille, U. *Chem. Eur. J.* **2002**, *8*, 340. (f) Dreessen, T.; Jargstorff, C.; Lietzau, L.; Plath, C.; Stademann, A.; Wille, U. *Molecules* **2004**, *9*, 480. (g) Jargstorff, C.; Wille, U. *Eur. J. Org. Chem.* **2003**, 3173. (h) Wille, U.; Jargstorff, C. *J. Chem. Soc., Perkin Trans. 1* **2002**, 1036. (i) Wille, U. *Tetrahedron Lett.* **2002**, *43*, 1239. (j) Wille, U. *J. Am. Chem. Soc.* **2002**, *124*, 14. (k) Stademann, A.; Wille, U. *Aust. J. Chem.* **2004**, *57*, 1055. (l) Sigmund, D.; Schiesser, C. H.; Wille, U. *Synthesis* **2005**, 1437.

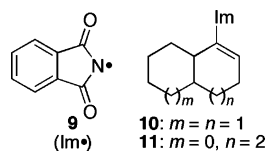


FIGURE 1. Reaction of imidyl radicals **9** with cycloalkyne leads to imidyl-substituted bicyclic alkenes **10** and **11** through a radical addition/cyclization sequence.

organic and inorganic *O*-centered radicals XO^{\bullet} (see Scheme 1 for the various *X*). Intrigued by the scope of this methodology, we therefore decided to examine the performance of other heteroatom-centered radicals in self-terminating radical reactions.

In an earlier paper we have demonstrated that the *N*-centered phthalimidyl radicals (Im $^{\bullet}$, **9**) do indeed react with cycloalkyne **1** through C–N bond formation to give imidyl-substituted bicyclic alkenes **10** and **11** (Figure 1).² These products are likely formed through a transannular HAT/*exo* radical cyclization sequence, e.g., **2b** \rightarrow **3b/4b** and **3b/4b** \rightarrow **5b/6b**, respectively, similar to that shown in Scheme 1 (with $YX^{\bullet} = \text{Im}^{\bullet}$). However, since homolytic cleavage of *N*-acyl bonds, in analogy to the terminating step in radical cyclizations involving *O*-centered radicals, seemed not to be an energetically favorable pathway for the radical intermediates **5b/6b**, the latter underwent stabilization through alternative mechanisms, which were not further explored.

Therefore, we reasoned that self-terminating radical cyclizations with *N*-centered radicals of type RXN^{\bullet} should be possible, if the substituent *X* would give a stable radical X^{\bullet} that is released through homolytic fragmentation of the N–*X* bond in the final step of the cyclization cascade shown in Scheme 1 (with *Y* = NR). In the case of cycloalkyne **1**, a successful self-terminating radical sequence should then lead to formation of the C=N double bond in the imines **7b** and **8b**. However, because of the intrinsic instability of imines,³ at least partial hydrolysis of the latter to the respective ketones **7a** and **8a** could also occur.

In this work we report on the performance of two different classes of *N*-centered radicals, e.g., aminium and amidyl radicals, in self-terminating radical cyclizations using the well-established reaction with the cyclic alkyne **1** as the model system. The experimental studies performed to reveal the synthetic scope of the concept are augmented by computational studies to obtain insights into the mechanism of the reactions under investigation.

Results and Discussion

Experimental Studies. Whereas neutral aminyl radicals preferably react with alkenes by HAT and are therefore not suitable for our purposes, *N*-protonation increases the electrophilicity of the radical center, and successful addition of aminium radicals to π systems has been reported in the literature.^{4,5} Compared with aminium radicals, amidyl radicals are less electrophilic. Although they are delocalized π -allyl

SCHEME 2

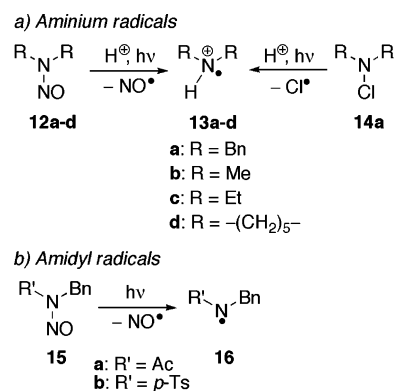


TABLE 1. Experimental Conditions and Results for the Reaction of Aminium Radicals **13a–d** with Cycloalkyne **1**^a

entry	[radical precursor]/mM	[1]/mM	solvent	acid	yield ^b /%
1	12a: 17	11	CH ₂ Cl ₂	0.1 M MA ^c	3
2	12a: 6	11	CH ₂ Cl ₂	0.1 M MA	31
3	12a: 9	11	CH ₂ Cl ₂	0.1 M TFA	7
4	12a: 13	9	CH ₂ Cl ₂	0.1 M HOAc	2
5	12a: 6	10	CH ₂ Cl ₂		0
6	12a: 8	11	MeCN	0.1 M MA	6
7	12a: 8	11	MeCN	0.1 M TFA	9
8	12a: 4	9	MeOH	1.25 M HCl	3
9	14a: 3	13	CH ₂ Cl ₂	0.1 M MA	10
10	14a: 24	11	MeCN	0.1 M TFA	31
11	12b: 21	6	CH ₂ Cl ₂	0.1 M TFA	61
12	12b: 32	8	MeCN	0.1 M TFA	57
13	12b: 10	8	MeCN	0.1 M MA	4
14	12b: 20	11	MeOH	1.25 M HCl	37
15	12b: 9	10	MeOH	1.25 M HCl	27
16	12c: 25	8	CH ₂ Cl ₂	0.1 M TFA	16
17	12c: 25	9	MeCN	0.1 M TFA	56
18	12d: 17	6	CH ₂ Cl ₂	0.1 M TFA	28
19	12d: 15	8	MeCN	0.1 M TFA	7

^a Mercury lamp (TQ150), 60 min, 10 mL of solvent. ^b Combined yield (based on minor compound) determined by GC using *n*-hexadecane as internal standard. ^c MA = malonic acid.

radicals, amidyl radicals react at nitrogen only.⁶ The aminium radicals **13a–d** were generated through photolysis of the respective *N*-nitrosoamines **12a–d** under acidic conditions. The dibenzylaminium radical **12a** was also photochemically generated from *N*-chloro amine **14a** (Scheme 2). The benzyl-substituted amidyl radicals **16a,b** were obtained through photolysis of the corresponding *N*-nitrosoamides **15a,b**. No indication for interfering reactions by nitric oxide or chlorine, the byproducts in the radical generation process, was found. All photochemical experiments were performed at least in duplicate.

Reaction of Aminium Radicals **13a–d with **1**.** In Table 1 are compiled the experimental conditions and results of the reaction of aminium radicals **13a–d** with **1**. The experiments were carried out on analytical scales by irradiating the radical precursor **12** in the presence of cycloalkyne **1** in the respective solvent/acid system (10 mL) for 60 min.⁷ After neutralization and workup, the reaction mixtures were analyzed by quantitative GC. For details see the Experimental Section.

(5) (a) Chow, Y. L. *Can. J. Chem.* **1965**, *43*, 2711. (b) Chow, Y. L. *Tetrahedron Lett.* **1964**, 2333. (c) Chow, Y. L.; Colon, C. *Can. J. Chem.* **1967**, *45*, 2559.

(6) Fossey, J.; Lefort, D.; Sorba, J. *Free Radicals in Organic Chemistry*; John Wiley & Sons/Masson: Chichester, UK, 1995.

(7) It was verified that **1** was completely consumed after 60 min of irradiation time.

(2) Wille, U.; Krüger, O.; Kirsch, A.; Lüning, U. *Eur. J. Org. Chem.* **1999**, 3185.

(3) Neale, R. S. *J. Org. Chem.* **1967**, *32*, 3263.

(4) Reviews on *N*-centered radicals: (a) Wolf, M. E. *Chem. Rev.* **1963**, *63*, 55. (b) Neale, R. S. *Synthesis* **1971**, 1. (c) Minisci, F. *Synthesis* **1973**, 1. (d) Chow, Y. L. *Acc. Chem. Res.* **1973**, *6*, 354. (e) Minisci, F. *Acc. Chem. Res.* **1975**, *8*, 165. (f) Chow, Y. L.; Danen, W. C.; Nelsen, S. F.; Rosenblatt, D. H. *Chem. Rev.* **1978**, *78*, 243. (g) Stella, L. *Angew. Chem., Int. Ed. Engl.* **1983**, *22*, 337.

The first experiments were performed using the dibenzylaminium radical **13a**, which was believed to perfectly satisfy the prerequisites for self-terminating radical cyclizations, since a stable benzyl radical should be released during the terminating homolytic bond scission (see Scheme 1; Y = NBn, X* = Bn[•]). Indeed, irradiation of a 60% excess of radical precursor **12a** in the presence of **1** in 0.1 M malonic acid (MA) in dichloromethane led to formation of the ketones **7a** and **8a** in, however, only very low yield (entry 1).⁸ Imines of types **7b** and **8b** were not found in any experiment in this study.⁹ Since there is no obvious alternative pathway for formation of the ketones **7a/8a**, other than through hydrolysis of imines **7b/8b** (or related species; see later), we consider ketone formation as indirect evidence for a successful radical addition/cyclization sequence. Using an excess of **1** resulted in an increase of the combined yield of **7a/8a** to about 31% (entry 2). Other solvents, e.g., acetonitrile or methanol, and other acids, e.g., trifluoroacetic acid (TFA), acetic acid, or hydrochloric acid, did not lead to a further improvement (entries 3, 4, and 6–8). No clear influence of the presence of oxygen on the yield was found (data not shown).

On the other hand, **7a/8a** were not formed in the absence of acid (entry 5). When **13a** was generated from the respective *N*-chloro amine **14a**, a similar outcome with regard to the yield of **7a/8a** was found, although the best solvent/acid system for this reaction was acetonitrile/0.1 M TFA (entries 9 and 10). During the irradiation of precursor **14a**, formation of significant amounts of *N,N*-dibenzylamine was observed. The different behavior of dibenzylaminium radicals **13a** in dependence of their precursor can be explained by the fact that radical generation through irradiation of *N*-nitrosoamine **12a** under acidic conditions occurs out of the protonated state leading directly to the aminium radical **13a**, whereas photolysis of *N*-chloro amine **14a** leads initially to aminyl radicals, which are protonated only in a subsequent step to yield **13a**.¹⁰ Obviously, under our conditions protonation of the aminyl radicals was competing with hydrogen abstraction (presumably from the solvent) to give *N,N*-dibenzylamine. Because of this side reaction, *N*-chloroamines were not further explored as a source for aminium radicals in this study.

To our surprise, the reaction of **1** with the aminium radicals **13b** and **13c** resulted in significantly higher combined yields of **7a/8a** of up to 61% (entry 11), or 56% (entry 17), respectively, although highly unstable alkyl radicals (methyl in the former, ethyl in the latter case) should be released in the final β -fragmentation step. Even the reaction of the cyclic piperidinium radical **13d** with **1** led to formation of **7a/8a** in an albeit moderate combined yield of 28% (entry 18), despite the fact that **13d** was deliberately chosen as representative for an *N*-centered radical possessing substituents with, at least what we believed, poor leaving group ability. Our unexpected result that no correlation between the stability of the leaving radical and the yield of oxidized products **7a/8a** was found leads to the question whether the assumed mechanism of the cyclization cascade is actually according to that shown in Scheme 1. We will address this in the second part of this paper.

(8) The ketones **7a** and **8a** were unambiguously identified by comparison of their GC retention times with those of authentic samples, in addition to GC/MS experiments.

(9) Attempts to trap *N*-containing intermediates, for example through in situ reduction of imines with sodium borohydride, were not successful.

(10) Cessna, A. J.; Sugamori, S. E.; Yip, R. W.; Lau, M. P.; Snyder, R. S.; Chow, Y. L. *J. Am. Chem. Soc.* **1977**, *99*, 4044.

TABLE 2. Experimental Conditions and Results for the Reaction of Amidyl Radicals **16a,b** with Cycloalkyne **1**

entry	[radical precursor]/mM	[1]/mM	solvent	yield ^a /% 7a + 8a
1	15a : 20	10	CH ₂ Cl ₂ ^{b,c}	7
2	15a : 20	10	CHCl ₃ ^{b,c}	6
3	15a : 20	10	cyclohexane ^{b,c}	traces
4	15a : 20	10	benzene ^{b,c}	11
5	15a : 20	10	MeOH ^{b,c}	traces
6	15a : 20	10	MeCN ^{b,c}	48
7	15a : 20	10	acetone ^{b,c}	52
8	15a : 20	10	MeCN ^{b,c,d}	65
9	15a : 20	10	MeCN ^{b,e}	35
10	15a : 80	40	MeCN ^{b,f}	17
11	15a : 20	10	MeCN ^g	47
12	15a : 40	10	MeCN ^g	42
13	15a : 10	10	MeCN ^g	17
14	15b : 20	10	MeCN ^{b,c}	38
15	15b : 20	10	acetone ^{b,e}	25
16	15b : 20	10	MeCN ^{b,c,d}	26
17	15b : 20	10	MeCN ^{c,h}	17
18	15b : 20	10	MeCN ^{c,d,h}	15
19	15b : 20	10	MeCN ^{c,i}	26
20	15b : 20	10	MeCN ^g	22

^a Combined yield (based on minor compound) determined by GC using *n*-hexadecane as internal standard. ^b Rayonet photoreactor at $\lambda = 350$ nm. ^c Reaction time 24 h. ^d Under O₂. ^e Reaction time 96 h. ^f Reaction time 48 h. ^g Mercury lamp (TQ150), reaction time 5 h. ^h Rayonet photoreactor at $\lambda = 300$ nm. ⁱ Rayonet photoreactor at $\lambda = 254$ nm.

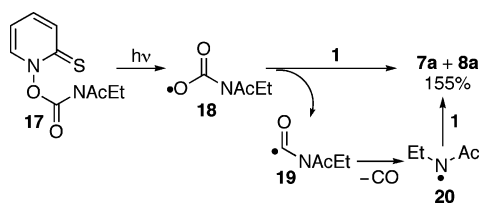
To conclude, the reactions of aminium radicals **13a–d** with **1** were highly inconclusive. Although the findings suggest that oxidative radical cyclizations with *N*-centered radicals should principally work, comparison of the various entries in Table 1 shows that optimized experimental conditions for the reaction of one radical, e.g., concentration ratio between alkyne and radical precursor, as well as the solvent and acid system, were not applicable to the reaction of a different radical (see, for example, entry 11 vs 16, entry 17 vs 19, etc.); in other words, the reaction conditions had to be re-optimized for each of the different radicals. Thus, in the case of radicals **13b–d** the highest yields of **7a/8a** were obtained with an excess of the respective radical precursor (entries 11, 17, and 18), but the opposite appeared to be the case with radical **13a** (entry 2). We cannot exclude, however, that the aqueous workup procedure, which was required to neutralize the reaction mixtures prior to analysis, led to secondary reactions, e.g., hydrolysis, etc., so that the observed GC data may not reflect the results of the radical reaction itself.¹¹

Reaction of Amidyl Radicals **16a,b with **1**.** In contrast to aminium radicals, self-terminating radical cyclizations with the amidyl radicals **16a** and **16b** could be performed under neutral conditions that allowed direct GC analysis of the reaction mixture without prior workup. The experimental conditions and results are compiled in Table 2. The reactions were also performed on analytical scales by irradiating the radical precursor **15** in the presence of cycloalkyne **1** in various solvents (5 mL) using either a mercury lamp or a Rayonet photoreactor at different wavelengths (e.g., $\lambda = 350$, 300, or 254 nm). The reaction mixtures were analyzed by quantitative GC and GC/MS. For details see the Experimental Section.

As before, also in the reactions of the amidyl radicals **16a,b** with **1**, the imines **7b/8b** were not formed, and the bicyclic ketones **7a** and **8a** were identified as exclusive products.⁹ We

(11) GC analysis of the crude, acidic reaction mixture was not possible.

SCHEME 3



believe that the latter must have been generated from the respective imines **7b/8b** or imine-type intermediates upon injection onto the GC column (we will discuss this possibility below).

Initial experiments were performed in which 2:1 mixtures of radical precursor **15a** and **1** in various solvents were irradiated for 24 h at $\lambda = 350$ nm in a Rayonet photoreactor. Generally, in contrast to the experiments with aminium radicals, the reactions with amidyl radicals appeared to be easier to control. Both acetonitrile and acetone were the best solvents, which often gave similar outcomes (because of this, Table 2 shows mostly the results of the experiments performed in acetonitrile), and combined yields of around 50% of **7a/8a** were obtained in the reaction of the acetamidyl radical **16a** with **1** (entries 6 and 7). Halogenated solvents, hydrocarbons, benzene, or methanol performed significantly poorer (entries 1–5). Elongation of the reaction time to 96 h (entry 9) and increasing the total concentration (entry 10) resulted in reduced yields. Using the stronger mercury lamp as a light source, an outcome similar to that in experiment 6 was obtained with an irradiation time of only 5 h (entry 11). A much larger excess of radical precursor **15a** (entry 12) does not affect the yield significantly, whereas an equimolar ratio of **15a** and **1** (entry 13) clearly resulted in a poorer outcome. Interestingly, the reaction performed in the presence of oxygen led to a significant increase of **7a/8a** formation (entry 8 vs 6).

Compared with **16a**, the tosylamidyl radical **16b**, which contained two suitable leaving groups with the tosyl radical supposedly being even more stable than the benzyl radical, gave generally lower yields of **7a/8a**. A maximum yield of 38% was found when the irradiation was performed in acetonitrile for 24 h at $\lambda = 350$ nm (entry 14). Longer reaction times (entry 15), shorter irradiation wavelengths (entries 17–19), or a different light source (entry 20) as well as the presence of oxygen (entries 16 and 18) only resulted in a reduction of the yield of **7a/8a**.

In a seemingly unrelated project, we became interested in studying the potential of carbamoyloxyl radicals in self-terminating radical oxygenations. Thus, when the *O*-centered radical **18**, which was generated through photolysis of the corresponding Barton ester **17** in acetonitrile,¹⁸ was reacted with excess cycloalkyne **1**, the bicyclic ketones **7a/8a** were obtained in a surprisingly high combined GC yield of 155% with respect to the radical precursor **17** (Scheme 3).

We suggest that after the first successful radical cyclization initiated by addition of **18** to **1** (see Scheme 1), the released carbamoyl radical **19** undergoes decarbonylation¹² to give the *N*-centered acetamidyl radical **20**. The latter subsequently reacts with **1** to yield further **7a/8a** after decomposition of the

intermediately formed imines **7b/8b** (or related intermediates; see below). Thus, although the released radical **19** from the first cyclization sequence does not act as a radical chain carrier, it undergoes transformation into a species that initiates a second cyclization cascade. We will be investigating further radicals exhibiting similar multistep activities in the future.

Computational Studies

Our experiments have clearly revealed that *N*-centered radicals can undergo addition to alkynes, where they initiate a radical cyclization sequence. However, since no apparent correlation between the stability of the leaving radicals and the yield of cyclized products, **7a/8a**, was found in the reaction of either aminium or amidyl radicals with **1**, the question arises, whether the mechanism of self-terminating radical cyclizations, as shown in Scheme 1 (which we believe is correct for *O*-centered radicals),¹³ is applicable to *N*-centered radicals. We have therefore performed computational studies to obtain a detailed mechanistic insight into the key steps in self-terminating radical cyclizations, particularly the initial addition of *N*-centered radicals to alkynes (**1** \rightarrow **2b**) and the terminating bond scission (**5b/6b** \rightarrow **7b/8b**).

The calculations were carried out using the Gaussian 03 program.¹⁴ Geometry optimizations were performed using the BHandHLYP/6-311G** and BHandHLYP/6-311++G** methods.¹⁵ The ground and transition states were verified by vibrational frequency analysis at the same levels of theory, and all identified transition states showed only one imaginary frequency. The spin expectation value, $\langle s^2 \rangle$, was very close to 0.75 after spin annihilation. The one-electron reduction potentials E° , absolute and relative to nonaqueous SCE, were calculated according to the procedure recently described by Coote et al.¹⁶ For this, the Gibbs free energy of each species was calculated at the BHandHLYP/6-311++G** level of theory (except for the half reaction in entry 5 of Table 6, for which the Gibbs free energy was computed at the BHandHLYP/6-31++G**) level, and the solvation energy was calculated using the conductor-like polarizable continuum model (CPCM) at the B3LYP/6-31+G* level of theory. All geometries of the studied species have been fully optimized in the gas phase at the BHandHLYP/6-311++G** level of theory and in the presence of solvent, i.e., acetonitrile, at the B3LYP/6-31+G* level of theory. The

(13) Dreessen, T. Ph.D. Thesis, Universität Kiel, 2004.

(14) Frisch, M. J.; Trucks, G. W.; Schlegel, H. B.; Scuseria, G. E.; Robb, M. A.; Cheeseman, J. R.; Montgomery, J. A., Jr.; Vreven, T.; Kudin, K. N.; Burant, J. C.; Millam, J. M.; Iyengar, S. S.; Tomasi, J.; Barone, V.; Mennucci, B.; Cossi, M.; Scalmani, G.; Rega, N.; Petersson, G. A.; Nakatsuji, H.; Hada, M.; Ehara, M.; Toyota, K.; Fukuda, R.; Hasegawa, J.; Ishida, M.; Nakajima, T.; Honda, Y.; Kitao, O.; Nakai, H.; Klene, M.; Li, X.; Knox, J. E.; Hratchian, H. P.; Cross, J. B.; Adamo, C.; Jaramillo, J.; Gomperts, R.; Stratmann, R. E.; Yazyev, O.; Austin, A. J.; Cammi, R.; Pomelli, C.; Ochterski, J. W.; Ayala, P. Y.; Morokuma, K.; Voth, G. A.; Salvador, P.; Dannenberg, J. J.; Zakrzewski, V. G.; Dapprich, S.; Daniels, A. D.; Strain, M. C.; Farkas, O.; Malick, D. K.; Rabuck, A. D.; Raghavachari, K.; Foresman, J. B.; Ortiz, J. V.; Cui, Q.; Baboul, A. G.; Clifford, S.; Cioslowski, J.; Stefanov, B.; Liu, G.; Liashenko, A.; Piskorz, P.; Komaromi, I.; Martin, R. L.; Fox, D. J.; Keith, T.; Al-Laham, M. A.; Peng, C. Y.; Nanayakkara, A.; Challacombe, M.; Gill, P. M. W.; Johnson, B.; Chen, W.; Wong, M. W.; Gonzalez, C.; Pople, J. A. *Gaussian 03*, Revision B.04; Gaussian, Inc.: Pittsburgh, PA, 2003.

(15) Single-point energy calculations performed with the QCISD/cc-pVDZ and CCSDT/cc-pVDZ methods on BHandHLYP/6-311G** and BHandHLYP/6-311++G** optimized geometries showed excellent agreement with results obtained from BHandHLYP/6-311G** and BHandHLYP/6-311++G** computations.

(16) Namazian, M.; Coote, M. L. *J. Phys. Chem. A* **2007**, *111*, 7227.

(12) The rate constants for decarbonylations are in the order 10^6 – 10^7 s^{-1} ; see for example: (a) Turro, N. J.; Gould, I. R.; Baretz, B. H. *J. Phys. Chem.* **1983**, *87*, 531. (b) Kurnysheva, O. A.; Gritsan, N. P.; Tsentlovich, Y. P. *Phys. Chem. Chem. Phys.* **2001**, *3*, 3677.

SCHEME 4

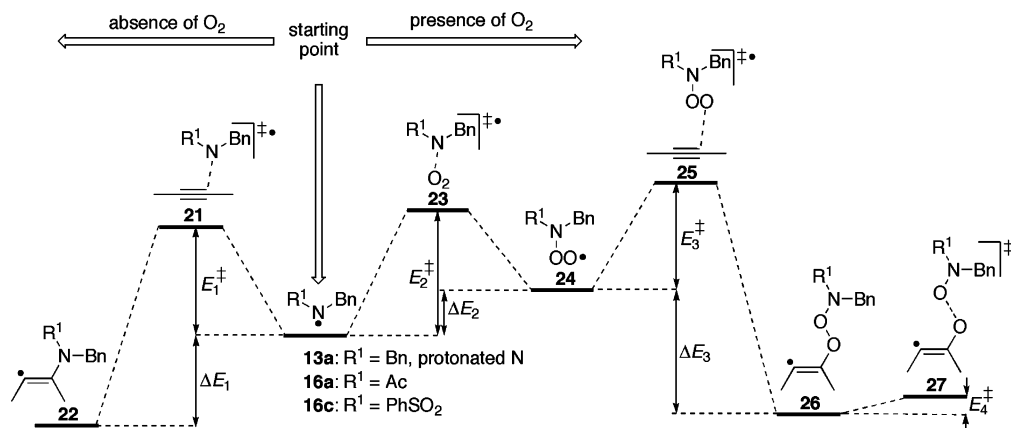


TABLE 3. Calculated Activation Energies, E^\ddagger , and Reaction Enthalpies, ΔE , for the Reaction of Acetamidyl Radicals **16a** with **1** (in kJ mol^{-1} ; BHandHLYP/6-311G**)^{a,b}

step	reaction	E^\ddagger	ΔE
1	1 + 16a → 2b	35.2	-80.7
		<i>40.8</i>	-66.3
2	2b → 4b (1,6-HAT)	29.6	-54.9
		<i>15.3</i>	-57.5
3	4b → 6b (6- <i>exo</i>)	35.1	-121.1
		<i>32.0</i>	-163.9
		129.9	24.5
4	6b → 8b + Bn^\bullet	<i>119.7</i>	8.2

^a Numbers in italics contain zero-point vibrational energy correction (ZPC). ^b Numbering of the reaction steps and intermediates is according to Scheme 1 (with R = Ac and X = Bn).

archive entries of the Gaussian output files for all optimized ground and transition state structures in this work are available as electronic Supporting Information.

To explore whether a self-terminating radical cyclization cascade is principally feasible with *N*-centered radicals, we investigated at first the potential surface of the reaction between **1** and the acetamidyl radical **16a** leading to the bicyclo[4.4.0]-decane derivative **8b** (see Scheme 1 with R = Ac and X = Bn). In Table 3 are compiled the calculated activation energies, E^\ddagger , and reaction enthalpies, ΔE , for each of the four reaction steps in the proposed mechanism. The data show that the entire reaction sequence is thermodynamically favorable with a total reaction energy ΔE_{total} of ca. -225 kJ mol^{-1} . Initial radical addition (step 1), transannular HAT (step 2), and transannular radical cyclization (step 3) have low E^\ddagger , and all three steps are strongly exothermic.¹⁷ In this sequence, the final homolytic bond cleavage is the only step associated with a significantly high E^\ddagger of some 130 kJ mol^{-1} (or ca. 120 kJ mol^{-1} with zero-point vibrational energy correction, ZPC, included), which is also slightly endothermic. However, compared with the ring opening **6b** → **4b** in reversal of the 6-*exo* cyclization, which requires not only around 150 kJ mol^{-1} but is also strongly endothermic, β -fragmentation **6b** → **8b** with release of a benzyl radical should principally be both the kinetically and thermodynamically more preferable pathway for intermediate **6b**.

Whereas the energetics of both transannular HAT and *exo* cyclization should not vary significantly with the nature of the *N*-substituent at the π system, it is very likely that activation

(17) Orienting computations have revealed that the energetics of the parallel pathway leading to the bicyclo[5.3.0]decane derivative **7b** via a 1,5-HAT and 5-*exo* cyclization are in the same order of magnitude.

TABLE 4. Calculated Activation Energies, E_1^\ddagger – E_4^\ddagger , and Reaction Enthalpies, ΔE_{1-3} , for the Addition of Aminium and Amidyl Radicals **13a** and **16a/c**, Respectively, to 2-Butyne in the Absence and Presence of Oxygen (in kJ mol^{-1} ; BHandHLYP/6-311G**)^a

entry	R ¹	E_1^\ddagger	ΔE_1	E_2^\ddagger	ΔE_2	E_3^\ddagger	ΔE_3	E_4^\ddagger
1	Bn ^b	28.0 ^c	-87.1	78.0	56.5	23.1	-39.8	8.9
		<i>32.7^c</i>	-69.1	86.6	72.3	24.4	-32.0	3.4
2	Ac	42.0	-91.1	54.3	-5.8	59.1	-24.0	2.8
		<i>49.1</i>	-74.4	61.1	9.4	63.5	-15.5	-2.0
3	PhSO ₂	55.1	-63.7	65.8	35.7	59.4	-20.1	11.0
		<i>57.6</i>	-51.9	69.6	45.8	61.1	-11.4	5.0

^a Numbers in italics contain zero-point vibrational energy correction (ZPC). ^b Protonated N. ^c Via an alkyne/radical association complex (see text).

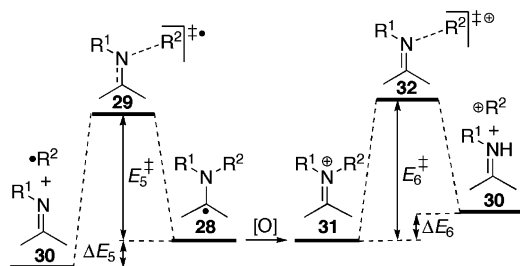
barrier and reaction enthalpy for the initial radical addition to the C≡C triple bond as well as for the terminating β -fragmentation are different for the various *N*-centered radicals used in this study. To get insight into the initial radical attack, calculations were performed on the addition of the aminium radical **13a** and amidyl radicals **16a** and **16c** (the latter mimics tosylamidyl radical **16b**) to alkynes in the absence and presence of oxygen, using 2-butyne as a simplified model for the cycloalkyne **1**. Scheme 4 shows the computed potential surface of these reactions, and the results of the calculations are listed in Table 4. At this point, we will focus the discussion on the radical addition in the absence of O₂.

Attack of the positively charged radical **13a** to 2-butyne proceeds via initial formation of a radical-alkyne association complex, with a low E_1^\ddagger of ca. 33 kJ mol^{-1} (entry 1, ZPC included),¹⁸ whereas E_1^\ddagger for the addition of amidyl radicals **16a** and **16c** to 2-butyne is 16–25 kJ mol^{-1} higher (entries 2 and 3).¹⁹ The reaction enthalpy ΔE_1 is strongly negative in all cases. Transition state **21** has *Z* geometry and leads initially to a *Z*-configured vinyl radical. In Table 4, ΔE_1 refers to an *E*-configured vinyl radical **22**. However, since the energy difference between *Z* and *E* vinyl radicals is generally not only minute but their interconversion requires also only few kJ mol^{-1} ,

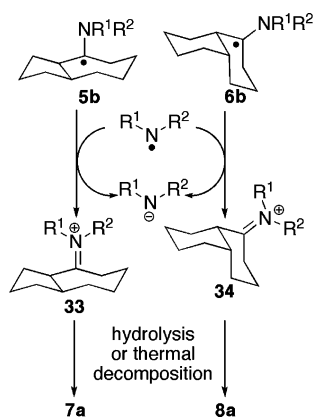
(18) The addition of **13a** to 2-butyne was found to have a negative activation barrier ($E_1^\ddagger = -11.5 \text{ kJ mol}^{-1}$, or -4.3 kJ mol^{-1} with ZPC included), which strongly suggests formation of an association complex between **13a** and 2-butyne prior to the actual radical addition. This complex was located on the potential surface and computed to be ca. 38 kJ mol^{-1} lower in energy than the free reactants.

(19) The lower E^\ddagger for the addition of **16a** to **1**, compared to the value calculated for addition of **16a** to 2-butyne (see Table 3), is believed to be due to release of ring strain in the ten-membered ring as a result of change in hybridization at the π bond from *sp* to *sp*² during the radical addition.

SCHEME 5



SCHEME 6



the error in ΔE_1 is negligible.^{6,20} Interestingly, the lower electrophilicity of the uncharged dibenzylaminy radical, compared with its protonated counterpart **13a**, is reflected by the finding that addition of the former to 2-butyne requires an activation energy that is higher by 60 kJ mol⁻¹ and less exothermic by ca. 55 kJ mol⁻¹ than **13a** (data not shown). It should be noted that an association complex between the uncharged amidyl radical **16a** and 2-butyne prior to addition was also located, but found to be only lower in energy by ca. 8 kJ mol⁻¹ compared to the free reactants. Because of this, we did not further pursue locating similar association complexes in the reactions of other uncharged radicals with alkynes.

After having established that addition of both aminium and amidyl radicals to C≡C triple bonds should be kinetically feasible reactions, we turned our attention to the terminating β -fragmentation. Using the simplified model system **28** for the actual radicals **5b/6b** (see Scheme 1), the transition state **29** for the homolytic cleavage of N–C bonds as well as of the product imine **30** and the released radical R^{2•} was calculated. The potential surface is shown in Scheme 5, and the results are compiled in Table 5.

As expected, the computations revealed that release of a benzyl radical from an amine-derived precursor **28** (entries 1–4) is both kinetically and thermodynamically significantly more favorable than release of an alkyl radical (entries 6–9, 11, and 12). The influence of basis sets augmented with diffuse functions on the outcome is not very large. It appears that E_5^\ddagger is usually reduced by 1–2 kJ mol⁻¹ when the BHandHLYP/6-311++G** method is used (entries 1 vs 2, 3 vs 4, and 8 vs 9), except for the cleavage of the methyl radical from the neutral **28** (entry 6 vs 7), where the augmented basis set resulted in a ca. 4 kJ mol⁻¹ higher value for E_5^\ddagger , compared to the 6-311G** basis. Generally, the BHandHLYP/6-311++G** method resulted in

TABLE 5. Calculated Activation Energies, E_5^\ddagger , and Reaction Enthalpies, ΔE_{5-6} , for the Homolytic and Heterolytic Bond Scission in **28** and **31**, Respectively (in kJ mol⁻¹)^a

entry	R ¹	R ²	E_5^\ddagger	ΔE_5	ΔE_6
1 ^b	Me	Bn	92.4	5.2	
			82.4	-10.9	
2 ^c	Me	Bn	90.7	0.6	
			80.6	-15.5	
3 ^{b,d}	Me	Bn	51.6	-17.0	
			41.1	-35.4	
4 ^{c,d}	Me	Bn	51.5	-21.0	
			40.7	-39.1	
5 ^c	Me	Bn			248.4
					229.2
6 ^b	Me	Me	124.4	64.7	
			110.8	40.4	
7 ^c	Me	Me	128.8	66.3	
			115.4	42.3	
8 ^{b,d}	Me	Me	104.9	36.7	
			90.6	10.0	
9 ^{c,d}	Me	Me	104.3	33.4	
			90.0	6.9	
10 ^c	Me	Me			548.3
					518.2
11 ^b	-(CH ₂) ₅ -		122.9	64.2	
			108.6	45.1	
12 ^b	-(CH ₂) ₄ -		114.9	54.6	
			102.4	38.7	
13 ^b	Ac	Bn	119.5	38.0	
			108.0	21.2	
14 ^b	Bn	Ac	161.5	114.9	
			154.2	100.2	
15 ^b	Ac	Me	158.3	95.5	
			143.2	68.2	
16 ^b	Ac	Ac	167.5	110.9	
			155.3	97.5	
17 ^b	Bn	PhSO ₂	32.9	-20.6	
			27.1	-29.5	
18 ^b	PhSO ₂	Bn	97.3	2.8	
			88.2	-11.8	

^a Numbers in italics contain zero-point vibrational energy correction (ZPC). ^b BHandHLYP/6-311G**. ^c BHandHLYP/6-311++G**. ^d Protonated N.

a more exothermic (or less endothermic, respectively) reaction by ca. 4 kJ mol⁻¹, and we therefore used this method for computing ΔE_6 for the heterolytic bond scission (see below).

Interestingly, homolytic cleavage of an N–C bond at a quarternary, protonated nitrogen, a very likely scenario under the acidic conditions in the experiments using aminium radicals, not only lowers E_5^\ddagger for release of a benzyl radical by ca. 40 kJ mol⁻¹ (entries 3 vs 1 or 4 vs 2) and for release of a methyl radical by ca. 25 kJ mol⁻¹ (entries 8 vs 6 or 9 vs 7), but also makes this cleavage process thermodynamically significantly more favorable. To conclude, of the various aminium radicals studied in this work, a successful termination of the radical cyclization sequence by homolytic β -fragmentation should only be possible with the dibenzylaminium radical **13a**.

The required energy for homolytic bond scission at an amide or imide nitrogen depends on the nature of the remaining substituent R¹. Generally, release of an acetyl radical is kinetically and thermodynamically even more unfavorable (entries 14 and 16) than release of a methyl radical (entry 15). Cleavage of a benzyl radical through fragmentation of an acetamide N–C bond (entry 13) requires some 20 kJ mol⁻¹ more energy than fragmentation of a sulfonamide N–C bond (entry 18). Of all the various β -fragmentations studied, the kinetically and thermodynamically most superior leaving group should be the phenylsulfonyl radical (entry 17), for which an

(20) Wille, U.; Dreessen, T. *J. Phys. Chem. A* **2006**, *110*, 2195.

TABLE 6. Calculated Reduction Potentials E° (in V), Using BHandHLYP/6-311++G** Gas-Phase Energies with Solvation Energies Obtained via CPCM Models, at the B3LYP/6-31+G* Level

Entry	Half reaction	E°	
		abs.	vs. SCE ^a
1		5.60	0.93
2		5.55	0.88
3		5.27	0.60
4		4.93	0.26
5 ^b		4.26	-0.41
6		4.22	-0.45
7		3.04	-1.63
8		2.97	-1.70
9		2.94	-1.73
10		2.83	-1.84

^a Versus nonaqueous SCE. ^b BHandHLYP/6-31++G** gas-phase energies.

E_5^\ddagger of only ca. 27 kJ mol⁻¹ and ΔE_5 of -30 kJ mol⁻¹ (ZPC included) were calculated at the BHandHLYP/6-311G** level of theory.

Although these computations unanimously support our perception of good or poor leaving groups in self-terminating radical reactions, they clearly contradict the experimental findings. This leads to the conclusion that the radical cyclizations investigated in this study cannot be terminated by a homolytic bond scission. As a mechanistic alternative, one could imagine that the radical intermediate **28** is oxidized by some means to the iminium ion **31** (we will discuss the nature of the oxidant below), which then undergoes heterolytic bond scission to give imine **30** with release of the substituent R² as a cation (see Scheme 5). However, computations of this alternative pathway showed that this process is highly endothermic for cleavage of both a benzyl and a methyl cation (Table 5, entries 5 and 10). A transition state could not be located. Calculations performed using a solvation model did not lower ΔE_6 significantly (data not shown). Therefore, such a heterolytic termination step can clearly be ruled out.

Because both radical and cationic terminations are an unlikely mechanism, how are the observed ketones **7a** and **8a** formed in our reactions? A possible pathway could involve the iminium ions **33** and **34**, respectively, which are hydrolyzed during aqueous workup, in the case of aminium radicals, or undergo thermal decomposition upon injection onto the GC column, in the case of amidyl radicals, to give **7a/8a** (Scheme 6). Formation of **33** and **34** could occur through oxidation of the α -nitrogen radical intermediates **5b** and **6b** by the respective electrophilic N -centered radical itself, which was usually present in excess (quantitative conversion of the radical precursor into the

respective N -centered radical is assumed). To explore this possibility, we calculated the reduction potentials, E° , both absolute and relative to nonaqueous SCE, for selected aminyl, aminium, and amidyl radicals as well as for simplified model systems of the α -nitrogen radical intermediates **5b/6b**, which are listed in Table 6.

The data show that the aminium radicals **13a** and **13b** are both good oxidizing agents (entries 1 and 2), whereas aminyl radicals are not (entries 9 and 10). Compared with aminium radicals, the amidyl radicals **16a** and **16c** (entries 3 and 4; the phenylsulfone residue was used as a simplified model for the tosyl residue in **16b**) have a slightly weaker oxidation capability. Most importantly, however, all aminium and amidyl radicals used in this study are thermodynamically capable of oxidizing their corresponding α -nitrogen radical intermediates to iminium ions (the respective redox systems are the half reactions 1 + 8, 2 + 7, 3 + 5, and 4 + 6 in Table 6). On the basis of these data, we conclude that the termination step in radical cyclization cascades initiated by addition of N -centered radicals to alkynes proceeds as proposed in Scheme 6 through oxidation of the radical intermediates **5b/6b** by the N -centered radicals themselves. Subsequent hydrolysis or thermal decomposition of the resulting iminium ions **33** and **34**, respectively, leads to the bicyclic ketones **7a/8a**. We believe that this redox pathway must be much faster than the homolytic N-C bond scission, and this would explain why a correlation between stability of the leaving group and yield was not found in our experiments.

Finally, we explored the role of oxygen in these reactions, especially the significant increase in yield of **7a/8a** in the reaction of amidyl radicals **16a** with **1** (see Table 2, entry 8). Because reaction of C -centered radicals with oxygen is a

convenient way to produce peroxy radicals,^{6,21} we wondered whether peroxy radical formation could also occur with *N*-centered radicals (see Table 4 and Scheme 4). Interestingly, the calculations show for amidyl radical **16a** that E_2^\ddagger required for formation of peroxy radical **24** (with $R^1 = \text{Ac}$) is higher by only ca. 12 kJ mol⁻¹ than E_1^\ddagger for addition of **16a** to 2-butyne (entry 2). Thus, although the former reaction appears to be kinetically less favorable than the latter, formation of peroxy radicals is a possible pathway, when one reaction partner, e.g., O₂, is present in large excess, which was the case in our experiments. The subsequent addition of **24** (with $R^1 = \text{Ac}$) to 2-butyne leads to a peroxyvinyl radical **26**. This radical addition requires an activation energy (E_3^\ddagger entry 2) similar to that required for the addition of sulfonamidyl radical **16c** to 2-butyne (E_1^\ddagger entry 3), which we know is feasible under our experimental conditions. The peroxy bond in vinyl radical **26** (with $R^1 = \text{Ac}$) is extremely labile, and γ -fragmentation to an α -oxo carbene (not shown) is a virtually barrierless process ($E_4^\ddagger = \pm 0$ kJ mol⁻¹). α -Oxo carbenes have been suggested as intermediates in the peroxide, dimethyldioxirane, and HOF·CH₃CN mediated epoxidation of **1**, which leads to formation of **7a/8a** through a stereoselective transannular 1,5 or 1,6 carbene C–H insertion reaction.²² Therefore, if under our experimental conditions a fraction of the amidyl radicals **16a** reacts with oxygen to produce ultimately α -oxo carbenes, two parallel pathways leading to formation of **7a/7b** are possible. In contrast to this, formation of peroxy radicals **23** through reaction of oxygen with dibenzylaminium radicals **13a** or sulfonamidyl radicals **16c**, respectively, is associated with a significantly higher activation barrier (E_2^\ddagger in entries 1 and 3) so that an α -oxo carbene pathway parallel to the direct addition of these radicals to the C≡C triple bond in **1** seems less likely.

Conclusions

This work was performed in order to explore whether the concept of self-terminating radical cyclizations of alkynes, which was discovered by us using *O*-centered radicals XO•, and which enables oxidation of alkynes to ketones under very mild conditions, could be extended to *N*-centered radicals RXN•, using the reaction with the cyclic alkyne **1** as a model system. Through a combination of experimental and computational studies, it was revealed that both aminium as well as amidyl radicals readily undergo intermolecular addition to the C≡C triple bond in alkynes, which triggers a series of intramolecular radical translocation and cyclization processes. However, in contrast to the homolytic fragmentation of the weak O–X bond with release of a radical X•, which occurs in the reaction of *O*-centered radicals with alkynes, computational studies revealed that the termination step in the case of *N*-centered radicals is an oxidative process, by which the isomeric iminium ions **33/34** are formed, which subsequently undergo hydrolytic or thermal decomposition to the corresponding ketones **7a/8a**. The

oxidant in these reactions is the *N*-centered radical itself. The reason for the different behavior of *O*- and *N*-centered radicals with regards to the termination step may be a combination of the relative ease to oxidize the α -nitrogen intermediates **5b/6b** and the difficulty to cleave N–C bonds in a homolytic fashion. Thus, the reaction of *N*-centered radicals with alkynes represents a highly interesting variation of self-terminating radical cyclizations, in which the radical addition/cyclization cascade is terminated by a redox process. The entire cascade allows oxidative transformation of alkynes into ketones under very mild conditions, and we will study the application of this methodology using other cyclic and open-chain alkynes in the future.

Whereas the conditions of the reactions involving amidyl radicals appeared to be easily controllable, the behavior of aminium radicals was very unpredictable and no general reaction conditions were found. In the case of the acetamidyl radical **16a**, a significant increase of the yield of **7a/8a** was found in the presence of oxygen. Computational studies lead to the suggestion that at least partial trapping of the *N*-centered radicals by oxygen is possible. The resulting peroxy radicals may then undergo addition to the C≡C triple bond to give a very labile vinyl radical that undergoes rapid γ -fragmentation to an α -oxo carbene. Subsequent transannular C–H insertion of the carbene may lead to formation of additional **7a/8a**, parallel to the pathway involving direct addition of the amidyl radical to the alkyne. Recently, we have reported on the first example of formation of α -oxo carbenes through γ -fragmentation in vinyl radicals,²³ and we are currently intensely exploring the scope of these reactions in our laboratory.

Experimental Section

1. Synthesis of the Radical Precursors. The compounds **12b–d** were commercially available. **12a**,²⁴ **14a**,²⁵ and **15b**²⁶ were prepared according to literature procedures.

***N*-Benzyl-*N*-nitrosoacetamide (15a).** (a) ***N*-Benzylacetamide:**²⁷ Triethylamine (76.6 mL, 0.55 mol) was added to a solution of benzylamine (54.6 mL, 0.5 mol) in THF (150 mL), the mixture was cooled to 0 °C, and acetylchloride (37.3 mL, 0.52 mol) in THF (50 mL) was slowly added. The reaction mixture was stirred for 3 h, warmed to rt, and quenched with saturated sodium bicarbonate solution (30 mL). The phases were separated and the aqueous layer was washed with dichloromethane (3 × 20 mL). The combined organic layers were dried over magnesium sulfate and concentrated. The crude product was purified by vacuum distillation (0.8 mbar, 138 °C) to give *N*-benzylacetamide as a yellowish solid (49.0 g, 66%). Mp 59 °C. ¹H NMR (CDCl₃, 400 MHz) δ 7.32–7.24 (m, 5H), 6.13 (s, broad, 1H), 4.38 (d, $J = 5.6$ Hz, 2H), 1.98 ppm (s, 3H). ¹³C NMR (CDCl₃, 100 MHz) δ 170.0, 138.1, 128.6, 127.7, 127.4, 43.6, 23.0 ppm.

(b) ***N*-Benzyl-*N*-nitrosoacetamide (15a):**²⁸ A solution of *N*-benzylacetamide (3.0 g, 0.02 mol) in a mixture of acetic acid (10 mL) and acetic anhydride (50 mL) was cooled to 0 °C, and sodium nitrite (3.04 g, 0.044 mol) was added over 1 h. The mixture was stirred at 0 °C until TLC indicated complete conversion (6 h), then the mixture was warmed to 10–15 °C, poured into ice/water, and extracted with diethyl ether (3 × 20 mL). The combined organic

(21) Alfassi, Z. P. *Chemistry of Free Radicals: Peroxy Radicals*; John Wiley & Sons: Chichester, UK, 1997.

(22) (a) Ciabattini, J.; Campbell, R. A.; Renner, C. A.; Concannon, P. *W. J. Am. Chem. Soc.* **1970**, *92*, 3826. (b) Dryuk, V. G. *Tetrahedron* **1976**, *32*, 2855. (c) Zeller, K.-P.; Kowallik, M.; Haiss, P. *Org. Biomol. Chem.* **2005**, *3*, 2310. (d) Curci, R.; Fiorentino, M.; Fusco, C.; Mello, R.; Ballistreri, F. B.; Failla, S.; Tomaselli, G. A. *Tetrahedron Lett.* **1992**, *33*, 7929. (e) Sun, S.; Edwards, J. O.; Sweigart, D. A.; D'Accolti, L.; Curci, R. *Organometallics* **1995**, *14*, 1545. (f) Murray, R. W.; Singh, M. J. *Org. Chem.* **1993**, *58*, 5076. (g) Espenson, J. H.; Zhu, Z. *J. Org. Chem.* **1995**, *60*, 7728. (h) Dayan, S.; Ben-David, I.; Rozen, S. *J. Org. Chem.* **2000**, *65*, 8816.

(23) Wille, U.; Andropof, J. *Aust. J. Chem.* **2007**, *60*, 420.

(24) Nakajima, M.; Warner, J. C.; Anselme, J.-P. *Tetrahedron Lett.* **1984**, *25*, 2619.

(25) Heuger, G.; Kalsow, S.; Göttlich, R. *Eur. J. Org. Chem.* **2002**, 1848.

(26) Overberger, C. G.; Anselme, J.-P. *J. Org. Chem.* **1963**, *28*, 592.

(27) Khan, A. T.; Choudhury, L. H.; Ghosh, S. *Eur. J. Org. Chem.* **2005**, 2782.

(28) Itoh, T.; Nagata, K.; Matsuya, Y.; Miyazaki, M.; Ohsawa, A. *Tetrahedron Lett.* **1997**, *38*, 5017.

phases were washed with water (30 mL), aqueous sodium carbonate (5%), and water (30 mL) and then dried over magnesium sulfate. The solvent was removed in vacuo, and the product was purified by flash chromatography (SiO₂, petroleum spirits/diethyl ether 3:1) to give **15a** as an orange liquid (2.70 g, 76%), which was stored under nitrogen at -30 °C. ¹H NMR (CDCl₃, 500 MHz) δ 7.26–7.18 (m, 5H), 4.92 (s, 2H), 2.79 (s, 3H). ¹³C NMR (CDCl₃, 100 MHz) δ 174.6, 134.6, 128.8, 128.0, 42.1, 22.8 ppm (1 overlapped arom. C).

2. Photochemical Radical Reactions. The irradiations were performed at 25–30 °C. A temperature associated with the reaction could not be observed under the experimental conditions. A dark reaction between the radical precursors and **1** could be strictly excluded in all cases.

(a) General procedure for the reaction of aminium radicals 13a–d with 1: **1** and the radical precursor (**12a–d** or **14a**) were dissolved in the respective solvent, and oxygen was removed by ultrasound treatment for 15 min under a steady flow of argon. The reaction mixture was irradiated using a mercury lamp for the given time under a steady flow of argon. After neutralization with saturated sodium bicarbonate solution, the phases were separated and the aqueous layer was washed with dichloromethane. The combined organic phases were dried over magnesium sulfate and concentrated. After the residue was dissolved in dichloromethane, a defined amount of *n*-hexadecane was added as internal standard for the subsequent analysis of the mixture by quantitative GC.

(b) General procedure for the reaction of amidyl radicals with 1: **1** was dissolved in the respective solvent, and oxygen was removed by ultrasound treatment for 30 min under a steady flow of nitrogen. The radical precursor (**15a,b**) was then added and the reaction mixture was irradiated using a mercury lamp or in a photoreactor for the given time under a steady flow of nitrogen. A defined amount of *n*-hexadecane was then added to the reaction mixture as internal standard, which was subsequently analyzed by quantitative GC.

Acknowledgment. This work was supported by the Australian Research Council under the Centre of Excellence program, Deutsche Forschungsgemeinschaft, Universität Kiel, Victorian Institute for Chemical Sciences High Performance Computing Facility, High Performance Computing Facility of the University of Melbourne, and the Australian Partnership for Advanced Computing.

Supporting Information Available: General experimental information and the archive entries of the Gaussian output files for all optimized geometries in this work. This material is available free of charge via the Internet at <http://pubs.acs.org>.

JO702261U